4712 *Macromolecules* **2009**, *42*, 4712–4718
DOI: 10.1021/ma900571d

Macromolecules
ARTICLE

Dielectric Relaxation of Polymer/Carbon Dioxide Systems

Yumi Matsumiya,[†] Tadashi Inoue,*[,‡] Tomohito Iwashige,[†] and Hiroshi Watanabe[†]

[†]*Institute for Chemical Research, Kyoto University, Uji, Kyoto 611-0011, Japan, and* [‡]*Department of Macromolecular Science, Graduate school of Science, Osaka University, 1-1 Machikaneyama, Toyonaka, Osaka 560-0043, Japan*

Received March 17, 2009; Revised Manuscript Received May 9, 2009

ABSTRACT: In general, pressurized CO_2 is soluble in polymers (to a concentration determined by the pressure) and affects the polymer relaxation behavior. Focusing on segmental relaxation, this study conducted dielectric measurements for racemic DL-poly(lactic acid) (PLA) as well as polystyrene (PS) under carbon dioxide (CO_2) pressurized up to $P_{CO_2} = 3.5$ MPa. The dielectrically detected segmental dynamics of PLA and PS was found to be accelerated on the increases of the CO_2 pressure P_{CO_2} that resulted in an increase of the CO_2 concentration (detected through a decrease of the dielectric intensity). In this sense, the pressurized CO_2 behaved as an ordinary solvent. However, the dielectrically detected segmental relaxation mode distribution was quite insensitive to P_{CO_2}, which was in strong contrast to the mode broadening induced by ordinary solvents such as di-*n*-butyl phthalate (DBP) (the broadening was confirmed also in this study for PLA plasticized with DBP). The mode broadening due to ordinary solvents is attributable to spatial fluctuation of the solvent concentration that results in a distribution of a local segment concentration, thereby giving a distribution of the segmental relaxation time, τ_s. Thus, the lack of this broadening seen for the PLA/CO_2 and PS/CO_2 systems strongly suggested lack of an effect of the CO_2 concentration fluctuation on the τ_s distribution. This unique feature of CO_2 was attributable to the motion of CO_2 molecules being much faster than the segmental motion of polymers: The fluctuation of CO_2 concentration was possibly smeared through the CO_2 motion before the dominant part of the segmental relaxation occurred, thereby giving no significant broadening of the τ_s distribution.

1. Introduction

Carbon dioxide (CO_2) is widely utilized in the field of polymer processing.[1,2] Pressurized CO_2 is considerably soluble in a variety of polymers and decreases their glass transition temperature (T_g). For a practical purpose, it is important to know the polymer rheology under pressurized CO_2. In fact, rheological measurements have been performed with pressure cells to reveal non-Newtonian flow behavior of polymers under fast shear.[3−7] However, it is also desired to investigate an effect of CO_2 on the polymer dynamics at equilibrium. This investigation requires dynamic experiments in the linear response regime. Linear viscoelastic moduli have been measured in a pressure cell mounted on a commercial rheometer,[8] but the accessible frequency range was very narrow so that only a limited aspect of the polymer dynamics has been elucidated.

For full investigation of the global dynamics of polymers governing the terminal relaxation/flow behavior at equilibrium, we recently conducted a dielectric test on polyisoprene (PI) under pressurized CO_2 up to $P_{CO_2} = 10$ MPa at 65 °C (which included the supercritical state of CO_2) and at frequencies ranging from 1 Hz to 10 MHz.[9] PI has the type A dipole parallel along the chain backbone and thus the test detected the end-to-end vector fluctuation, the motion over the maximum length scale of the chain. This motion was found to be accelerated while its mode distribution was not affected by pressurized/dissolved CO_2 even for a case of CO_2 in the supercritical state. In other words, CO_2 was found to behave as an ordinary solvent (or plasticizer) for the global motion of PI.

This fact naturally leads to an expectation that the pressurized CO_2 behaves as an ordinary solvent/plasticizer also for the local, segmental dynamics. Thus, we have conducted dielectric measurements for racemic DL-poly(lactic acid) (PLA) and polystyrene (PS) to examine this expectation. The pressurized CO_2 was found to accelerate the segmental relaxation without affecting the mode distribution. This effect of pressurized CO_2 on the segmental relaxation was in strong contrast to the effect of ordinary solvents (under ambient pressure), the acceleration associated with the mode broadening. This paper presents details of these results and discusses this unique behavior of pressurized CO_2 (lack of broadening effect on the segmental dynamics) in relation to the motion of CO_2 molecules.

*Corresponding author. E-mail: tadashi@chem.sci.osaka-u.ac.jp.

2. Experimental Section

2.1. Materials. Racemic DL-polylactic acid (PLA) (M_w = 20 000, M_w/M_n = 1.8) and the standard polystyrene (PS) (M_w = 37 900, M_w/M_n = 1.01) were purchased from Wako Co. Ltd. and Tosoh Co. Ltd., respectively, and used as received. The segments of PLA and PS have so-called type B dipoles perpendicular to the chain backbone (cf. Figure 1), and thus their motion results in the dielectric dispersion (α-relaxation). (PLA also has the type A dipole parallel along the chain backbone,[10] and its global chain motion is dielectrically active. However, this study focuses on the segmental relaxation at relatively high frequencies where the global relaxation is too slow to be detected.)

Carbon dioxide (CO_2) was purchased from Kyoto Teisan Co. Ltd. and used as received. The tank of CO_2 was directly connected, through a pressure regulator, to a pressure cell for the dielectric measurements. (cf. Figure 2).

Di-*n*-butyl phthalate (DBP, density = 1.04 g/cm^3), utilized as an ordinary solvent/plasticizer, was purchased from Wako Co. Ltd. and used as received. Two PLA/DBP mixtures (solutions)

 Published on Web 06/17/2009

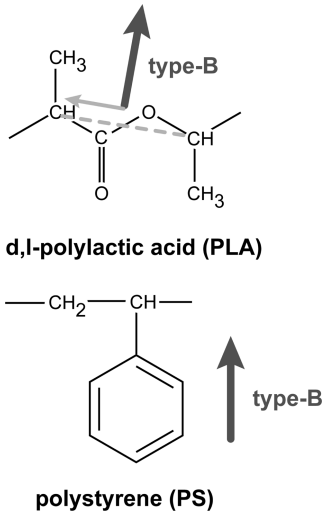

Figure 1. Schematic illustration of chemical structure and dipole of (a) poly(lactic acid) and (b) polystyrene.

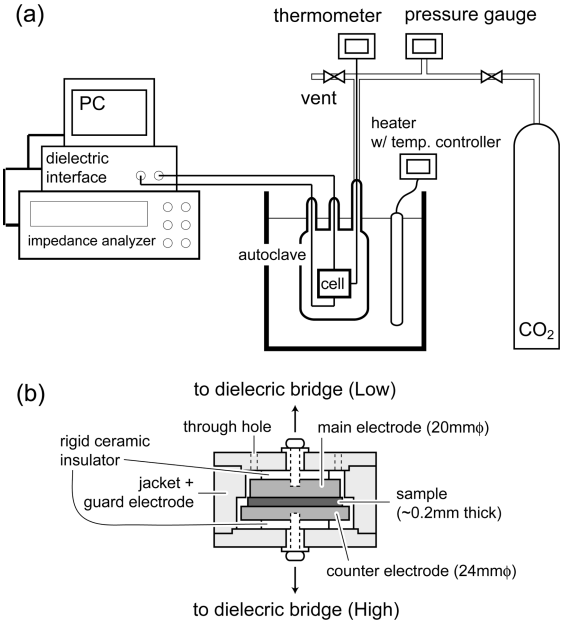

Figure 2. Schematic illustration of (a) the dielectric setup and (b) side view of the dielectric cell.

were prepared by dissolving prescribed masses of PLA and DBP into benzene and then allowing benzene to thoroughly evaporate at ambient atmosphere. The DBP concentration in these mixtures, 4 and 12 wt %, was determined from the mass of the mixtures after this evaporation.

2.2. Measurements. Linear viscoelastic measurements were conducted for the PLA sample with a vibrating tensile rheometer (Rheospectoler DVE3, Rheology Co., Ltd., Kyoto, Japan). The heat-pressed PLA plate of ca. 0.5 mm thickness was cut into a strip of the size of 5 mm×30 mm. Storage and loss Young's moduli, E' and E'', were measured as a function of frequency f at an ambient atmospheric pressure. Frequency sweep measurements were performed for frequencies from 1 to 130 Hz at the temperatures in a range between a temperature slightly above T_g to a softening temperature.

Dielectric measurements were conducted for the PLA and PS samples under pressurized CO_2 as well as the neat PLA and PS samples and PLA/DBP mixtures without pressurized CO_2. Parts a and b of Figure 2 illustrate the dielectric setup and the dielectric cell, respectively. An impedance analyzer (1260, Solartron) connected with a dielectric interface (1296, Solartron) was utilized together with homemade dielectric cells (having a porous gas inlet for the measurement under CO_2 pressure); more details of the dielectric setup were reported elsewhere.[9]

For the dielectric measurements under pressurized CO_2, a sample film (ca. 0.5 mm thick) was cut into a round disk equal sized to the main electrode (20 mm in diameter). The disks of PLA and PS were heated to 48.5 and 110 °C (= 1.6 and 10 °C above respective T_g at ambient pressure), sandwiched between the electrodes, squeezed (at those temperatures) to a thickness of ca. 0.2 mm. Then, the pressurized CO_2 was introduced, and the sample in the cell was dielectrically monitored until the CO_2 dissolution therein was saturated to achieve equilibrium. This saturation/equilibration required 2 days and 0.5 day for PLA and PS, respectively, as noted from disappearance of a time-dependent change of the dielectric response (at frequencies f/Hz between 10^{-2} and 10^6) monitored once in every 1 h. For the PLA and PS samples thus equilibrated under the pressured CO_2 as well as the PLA/DBP sample, frequency sweep tests were performed at frequencies f/Hz between 10^{-2} and 10^6 (between 0.62 and 6.2×10^7 for angular frequency $\omega = 2\pi f$) and at the applied electric field of 1.5 V/mm (in the linear response regime). No chemical degradation was detected with gel permeation chromatography for the materials recovered after the dielectric measurements.

The complex capacitance obtained from the frequency sweep test, $C^*(\omega) = C'(\omega) - iC''(\omega)$ ($i^2 = -1$), is expressed in terms of the material property and geometrical parameters as

$$C^*(\omega) = \varepsilon_v \varepsilon^*(\omega) \frac{A}{L} \tag{1}$$

where ε_v and $\varepsilon^*(\omega)$ are the absolute dielectric permittivity of vacuum (= 8.854 pF m^{-1}) and the (relative) dielectric permittivity of the material of our interest, respectively. A and L are the area of the main electrode (upper electrode shown in Figure 1b; $A = 3.14 \times 10^{-4}$ m^2) and the gap between electrodes (= 0.2 mm as determined from the empty cell capacitance described below).

Prior to the dielectric measurements, the capacitance of the empty cell, $C_0^*(\omega) = C_0'(\omega) - iC_0''(\omega)$, was determined at various temperatures T and CO_2 pressures P_{CO_2}. $C_0'(\omega)$ was independent of ω (though slightly changed with T and P_{CO_2}) while $C_0''(\omega)$ was negligibly small in a range of ω of our interest. The empty cell capacitance thus obtained, C_0 (= 14 pF), was utilized to determine the dynamic dielectric constant ε' and dielectric loss ε'', the real and imaginary components of ε^* ($= \varepsilon' - i\varepsilon''$), as

$$\varepsilon'(\omega) = \frac{C'(\omega)}{C_0}, \quad \varepsilon'(\omega) = \frac{C''(\omega)}{C_0} \tag{2}$$

The decrease of the dynamic dielectric constant, $\varepsilon_0 - \varepsilon'$ with $\varepsilon_0 = [\varepsilon']_{\omega \to 0}$ (static dielectric constant), and the dielectric loss ε'' are expressed in terms of the dielectric relaxation spectrum $L(\lambda)$ (with λ being the relaxation time) as[11] $\varepsilon_0 - \varepsilon' = \int_{-\infty}^{\infty} L(\lambda)\omega^2\lambda^2/\{1 + \omega^2\lambda^2\}$ d ln λ and $\varepsilon'' = \int_{-\infty}^{\infty} L(\lambda)\omega\lambda/\{1 + \omega^2\lambda^2\}$ d ln λ. This expression is formally identical to the expression of the moduli, E' and E'', in terms of the viscoelastic spectrum. Thus, the molecular dynamics in the samples is most clearly examined for the set of $\varepsilon_0 - \varepsilon'$ and ε'' data.

3. Results and Discussion

3.1. Viscoelastic and Dielectric Relaxation of PLA under Atmospheric Pressure. Figure 3a shows the viscoelastic E' and E'' and dielectric $\varepsilon_0 - \varepsilon'$ and ε'' data of PLA at ambient atmospheric pressure (no CO_2 pressure). We applied the time−temperature supposition to the data at various temperatures and reduced them at a reference temperature, T_r = 48.5 °C (= T_g + 1.6 °C). The shift factor a_T utilized for this

reduction is shown in Figure 3b. Time−temperature superposition works well for both of the viscoelastic and dielectric data, and the shift factors for those data are very close to each other and well described the WLF equation (solid curve in Figure 3b):

$$\log a_T = -\frac{13.3(T - T_r)}{44.5 + T - T_r} \quad (3)$$

In Figure 3a, the glassy region of E' ($\sim 10^9$ Pa), seen at angular frequencies $\omega > 10^2$ s^{-1}, is followed by the glass-to-rubber transition region at lower ω down to 10^{-2} s^{-1} where E' is larger than E'' and both of E' and E'' decrease to the order of 10^6 Pa. For many polymers, the ε'' peak for the segmental relaxation (detected through the motion of type B dipoles) is observed at a frequency that is $\sim$2 orders of magnitude lower than the corresponding E'' peak frequency.[12] (This difference between the ε'' and E'' peaks partly reflects a difference between relaxation and retardation spectroscopies, the latter involving the dielectric spectroscopy, and also a difference of the segment sizes giving the most intensive viscoelastic and dielectric dissipations.) The ε'' peak for PLA is observed right at such a frequency, allowing us to identify the dielectric relaxation seen in Figure 3b as the segmental relaxation (α-relaxation corresponding to the glass transition).

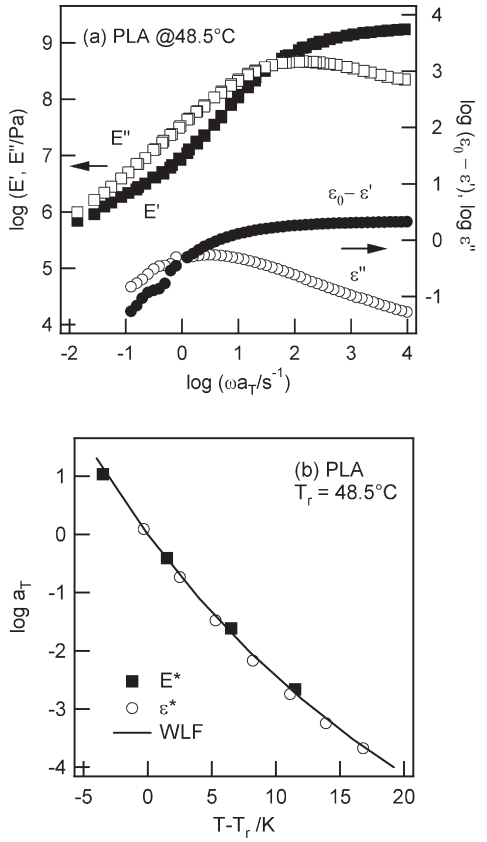

Figure 3. (a) Storage and loss Young's moduli, E' and E'' (filled and unfilled squares), and decrease of dynamic dielectric constant and dielectric loss, $\varepsilon_0 - \varepsilon'$ and ε'' (filled and unfilled circles), measured for PLA under ambient atmospheric pressure at 48.5 °C. The data are plotted against the angular frequency ω. (b) Time−temperature superposition shift factor a_T for PLA as a function of temperature $T - T_r$, where the reference temperature T_r is set at 48.5 °C.

3.2. Overview of Dielectric Behavior of PLA under Pressurized CO_2. Figure 4 shows dielectric behavior of PLA equilibrated at 48.5 °C under various CO_2 pressures, $P_{CO_2} = 0$, 0.54, 1.08, 1.56, and 2.02 MPa. In the experiment, we increased P_{CO_2} in a stepwise way and measured the data at each P_{CO_2} after monitoring the dielectric signal with time (for 5−48 h) and confirming the equilibration (no time-dependent change of the signal). The data for $P_{CO_2} = 0$ were measured in vacuum, and they were indistinguishable from the data obtained under ambient atmospheric pressure. The CO_2 molecule is a linear molecule and has no permanent dipole (thereby exhibiting just fast relaxation due to atomic/electronic displacement not detected in our experimental window). The segmental relaxation of PLA, followed by the direct current (dc) conduction giving $\varepsilon'' \propto \omega^{-1}$ at low ω, is clearly observed in our experimental window. This relaxation shifts to higher ω with increasing P_{CO_2}, indicating that the pressurized CO_2 is dissolved in PLA to give the plasticization effect on the segmental relaxation. A small decrease of the ε'' peak height with increasing P_{CO_2}, being equivalent to a decrease of the dielectric intensity, reflects the decrease of PLA concentration on this dissolution of CO_2.

Here, a comment needs to be added for the above data obtained after the stepwise increases of P_{CO_2}. A reviewer for this paper posed a question if the data were reproduced in a reverse experiment of decreasing P_{CO_2}. It was rather difficult to conduct this reverse experiment because CO_2 bubbles easily formed in the material on the stepwise decrease of P_{CO_2}. However, we confirmed that careful/slow release of the CO_2 pressure reproduced the PLA data at the lower pressure. This fact, together with the long equilibration time waited in the "stepwise increase" experiment, suggests that the data shown in Figure 4 can be safely regarded as the equilibrium data.

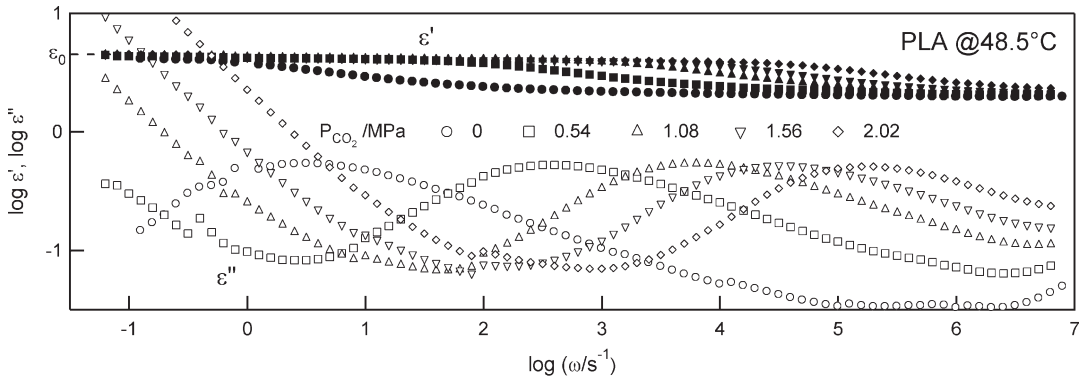

Figure 4. Dynamic dielectric constant and dielectric loss, ε' and ε'' (filled and unfilled symbols), measured for PLA at 48.5 °C equilibrated under various CO_2 pressures.

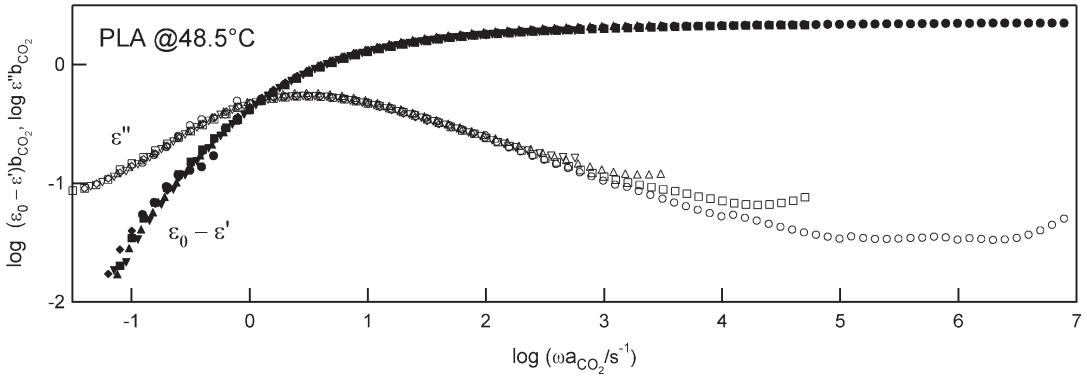

Figure 5. Time−CO_2 pressure superposition of $\varepsilon_0 - \varepsilon'$ and ε'' data (filled and unfilled symbols) measured for PLA at 48.5 °C.

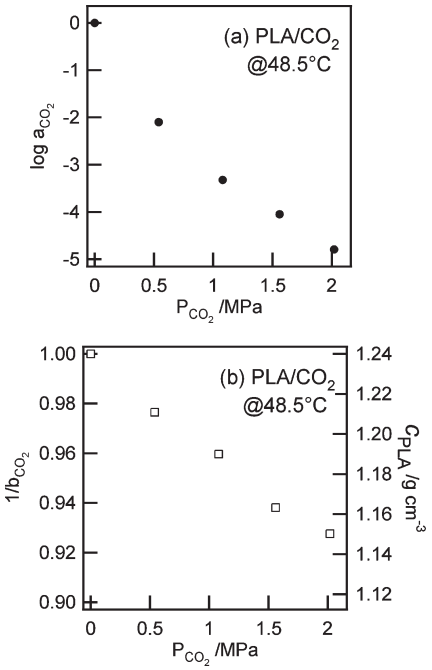

Figure 6. (a) Lateral shift factor, a_{CO_2}, utilized for the time−CO_2 pressure superposed master curve of the dielectric data shown in Figure 5. This shift factor is plotted against CO_2 pressure P_{CO_2}. (b) Reciprocal of the vertical shift factor, $1/b_{CO_2}$, plotted against CO_2 pressure P_{CO_2}. The mass concentration of PLA c_{PLA} evaluated from the $1/b_{CO_2}$ factor is also shown; see right axis. For more details, see text.

Figure 5 shows time−pressure superposed master curves of the $\varepsilon_0 - \varepsilon'$ and ε'' data of PLA shown in Figure 4. The data in the dc conduction regime are located at lower ω not covered in Figure 5. Figure 6 shows the horizontal and vertical shift factors, a_{CO_2} and b_{CO_2}, giving the excellent superposition shown in Figure 5. Since the dielectric mode distribution does not change with P_{CO_2} (cf. Figure 5), the magnitude of plasticization (approximately a decrease of effective T_g) is quantified by a_{CO_2} while a decrease of the dielectric intensity $\Delta\varepsilon$ is specified by b_{CO_2}. This decrease of $\Delta\varepsilon$ reflects a decrease of the PLA concentration on dissolution of CO_2, as explained in the next section.

3.3. Estimation of PLA/CO_2 Concentration. Sorption of CO_2 in polymers and the resulting dilation have been studied with various methods.[1,2] For example, a magnetic suspension balance (MSB) is frequently used to determine the amount of CO_2 sorption.[5,6] The buoyancy of the cell should be calibrated by the net weight of the polymer/CO_2 mixture, which requires *PVT* data of the polymer and CO_2 density. Moreover, to obtain the solubility of CO_2 to the polymer, the swollen volume of the polymer is required, which could not be measured directly. Thus, models such as Sanchez−Lacombe equation-of-state are utilized. The Sanchez−Lacombe model is often employed[3,5,6,14] and is known to work excellent for polymers such as high-density polyethylene, but not that good for rubbers like polyisoprene. Thus, the precise determination of polymer concentration under pressurized CO_2 is still a challenge. However, fortunately, the *PVT* data for PLA are available.[14] Here, we examine the dielectric estimate of the PLA concentration by comparing this estimate with the concentration evaluated from the *PVT* data.

The dielectric intensity $\Delta\varepsilon$ is expressed in terms of several molecular parameters as[13]

$$\Delta\varepsilon = Fg\nu\frac{\mu^2}{3k_B T} \tag{4}$$

Here, F is Onsagar factor having a value of the order of unity, μ is the dipole moment, k_B is the Boltzmann constant, T is the absolute temperature, and ν is the number density of the dipoles. g is the Kirkwood−Fröhlich factor that represents motional correlation of the dipoles. We may safely assume that F and g are insensitive to the existence CO_2. Then, from eq 4, a ratio of the mass concentration c of PLA in the presence of the pressurized CO_2 to the mass density ρ of neat PLA in a reference state at $P_{CO_2} = 0$ ($\rho_{ref} = 1.24$ g/cm^3)[14] is expressed in terms of the dielectric intensity $\Delta\varepsilon$ and the vertical shift factor b_{CO_2} as

$$\frac{c}{\rho_{ref}} = \frac{\Delta\varepsilon}{\Delta\varepsilon_{ref}} = \frac{1}{b_{CO_2}} \tag{5}$$

The dielectric mode distribution of PLA does not change with P_{CO_2} (cf. Figure 5) so that its $\Delta\varepsilon/\Delta\varepsilon_{ref}$ ratio coincides with reciprocal of the vertical shift factor for the data measured at the same T.

Figure 6b shows plots of this $1/b_{CO_2}$ factor against P_{CO_2}. Clearly, $1/b_{CO_2}$ decreases linearly with increasing P_{CO_2}, and the c_{PLA} decreases accordingly (cf. scale on the right axis). For example, at $P_{CO_2} = 2.02$ MPa, we obtain a dielectric estimate of $c_{PLA} = c_{ref}/b_{CO_2} = 1.15$ g/cm^3 ($1/b_{CO_2} = 0.93$). This result is consistent with a volume expansion ratio for PLA swollen with CO_2, $r_V \cong 1.05$ at $P_{CO_2} = 2$ MPa and $T = 40$ °C, measured by Liu and Tomasko:[14] This r_V value is unequivocally converted to the mass concentration, $c = \rho_{ref}/r_V = 1.18$ g/cm^3, which satisfactorily agrees with our dielectric estimate. If the partial specific volume of PLA does not change with P_{CO_2}, the PLA and CO_2 volume fractions are obtained from our c_{PLA} value as $\phi_{PLA} = c_{PLA}/\rho_{ref} = 0.93$ and $\phi_{CO_2} = 1 - \phi_{PLA} = 0.07$ at $P_{CO_2} = 2.02$ MPa and $T = 48.5$ °C.

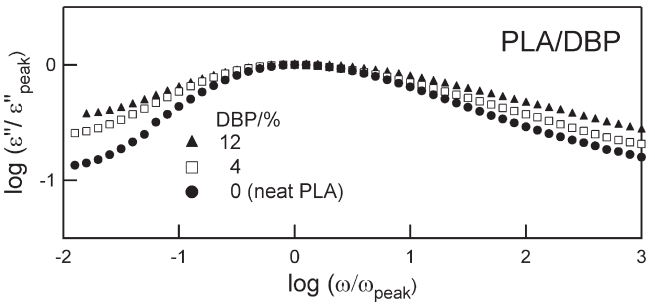

Figure 7. Comparison of dielectric loss data of neat PLA and PLA plasticized by dibutyl phthalate (DBP). These data are normalized at the loss peak.

Here, a comment should be added about the volume change (swelling) of PLA sample due to dissolution of CO_2 and its effect on the dielectric measurement. The swelling surely occurred to the volume expansion ratio, for example, to $r_V \cong \rho_{ref}/c = 1.05$ at $P_{CO_2} = 2$ MPa and $T = 40$ °C as reported in the literature.[14] However, our dielectric cell had rigidly fixed electrodes with a constant gap, and the PLA sample was already a molten liquid at $T = 48.5$ °C ($> T_g$) in our experiment when CO_2 was introduced in the cell. Thus, the increased volume of the material should have flowed out from the gap between the electrodes and stayed out of the main electrode (cf. Figure 2b). This flow-out material does not contribute to the dielectric signal detected with the main electrode, meaning that the swelling of our PLA sample did not affect the dielectric data.[15]

3.4. Dielectric Mode Distribution of Segmental Relaxation. For bulk polymers, the segment size has been estimated from viscoelastic data at high frequencies with the aid of the modified stress-optical rule.[16] This size was found to be close to that of the Kuhn segment size.[16] In contrast, the segment size has been hardly estimated from the dielectric data partly because this estimation requires us to know the effective dipole per segment, but this "dielectrically detected" segment may be similar, in size, to the "viscoelastically detected" segment (approximately Kuhn segment). For either viscoelastic or dielectric relaxation, it is well established that *cooperative* motion of the segments determines the segmental relaxation time and mode distribution.[11,12]

The dielectric mode distribution of the segmental relaxation is known to broaden on dilution with ordinary solvents.[17−19] This broadening is partly attributable to a spatial fluctuation of the solvent concentration[17−19] (which results in a distribution of segmental friction) as well as to an increase of the segment size on dilution.[20]

Thus, the lack of the mode broadening observed for PLA diluted (plasticized) by CO_2 (Figure 5) is quite different from the behavior of polymers diluted with ordinary solvents. One may argue that this peculiar behavior of the PLA/CO_2 system reflects specific features of either PLA or CO_2 (or both). To test this point, we chose di-*n*-butyl phthalate (DBP) and polystyrene (PS) as representative examples of ordinary solvents and nonpolar polymers, respectively, and examined the dielectric behavior of PLA/DBP and PS/CO_2 systems. The results are summarized below.

Figure 7 shows the dielectric loss ε'' measured in the segmental relaxation regime for PLA/DBP systems. For clear observation of changes in the mode distribution, the data are normalized at the ε'' peak. The weight fractions of DBP in the PLA/DBP systems are 4 and 12 wt %, and the corresponding DBP volume fraction (evaluated on the basis of an assumption of volume additivity), 4.9 and 14.5 vol %, is of the same order of magnitude as the CO_2 volume fraction

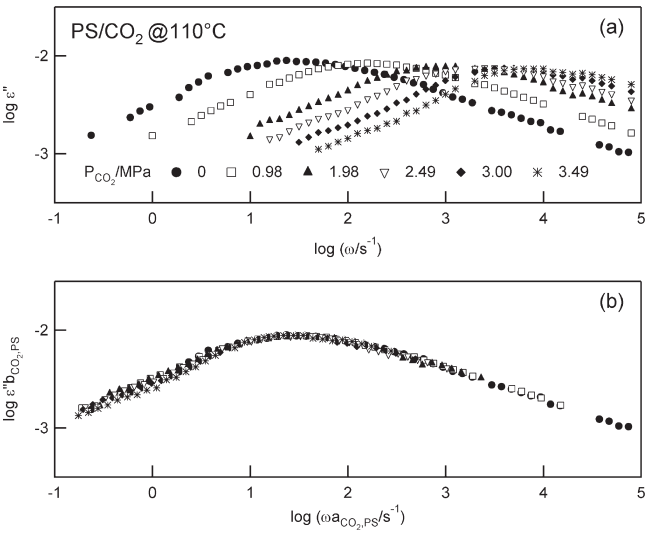

Figure 8. (a) Frequency dependence of dielectric loss of polystyrene (PS) at 110 °C equilibrated under various P_{CO_2}. (b) Time−CO_2 pressure superposed master curve of the dielectric loss.

(≤ 7 vol %) in the PLA/CO_2 system examined in Figure 5. Clearly, DBP at that volume fraction broadens the dielectric mode distribution of segmental relaxation of PLA, which makes a contrast to the effect of CO_2.

Figure 8a shows the ε'' data measured in the segmental relaxation regime (at 110 °C) for the PS/CO_2 system. The CO_2 pressure P_{CO_2} was varied from 0 (in vacuo) to 3.49 MPa. The segmental relaxation is accelerated with increasing P_{CO_2}, as similar to the behavior of the PLA/CO_2 system. The time−pressure superposition worked well for the ε'' data of the PS/CO_2 system to give the master curve shown in Figure 8b, and the lateral and vertical shift factors $a_{CO_2,PS}$ and $b_{CO_2,PS}$ giving this superposition are summarized in Figure 9a,b. The $b_{CO_2,PS}$ data for PS are in the same range as the $b_{CO_2,PLA}$ data for PLA (Figure 6b), and PS was swollen with CO_2 to an extent similar to that for PLA was. Thus, the PLA and PS samples similarly swollen with CO_2 exhibit no broadening of their segmental relaxation.

Comparison of Figures 5, 7, and 8 strongly suggests that the acceleration of segmental relaxation without the mode broadening is related to a specific feature of the pressurized CO_2. In relation to this point, one might argue that the high pressure itself could affect the mode distribution. In fact, for polyisoprene compressed with silicone oil, the segmental relaxation is retarded and slightly broadened when the pressure is increased up to 300 MPa.[21] However, the CO_2 pressure applied in this study is much smaller ($P_{CO_2} \leq 3.49$ MPa; cf. Figures 4 and 8), enabling us to safely neglect this pressure effect and relate the lack of mode broadening exclusively to the feature of CO_2.

Since the acceleration of the segmental relaxation due to CO_2 is similar to the plasticization effect observed for ordinary solvents (including DBP examined in Figure 7), CO_2 appears to provide an extra space, or free volume, with the polymer segments to accelerate their motion (as ordinary solvents do). The concentration fluctuation of ordinary solvents gives a frictional distribution for the segments to broaden the mode distribution. CO_2 is not a very good solvent for PLA and PS, and its concentration should have fluctuated also in these systems. However, the CO_2 motion could be much faster than the motion of ordinary solvents, and the concentration fluctuation may be smeared through such fast motion of CO_2 in a time scale shorter than that for

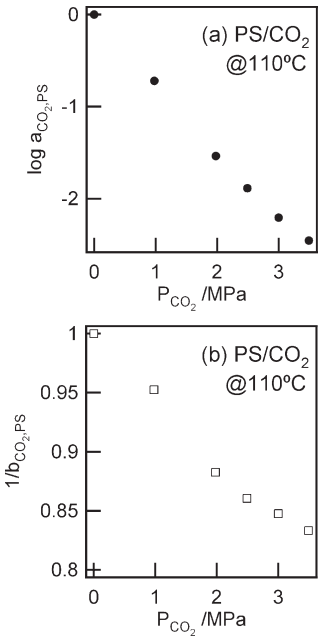

Figure 9. (a) Lateral shift factor, $a_{CO_2,PS}$, utilized for the time−CO_2 pressure superposed master curve of the dielectric data shown in Figure 8. This shift factor is plotted against CO_2 pressure P_{CO_2}. (b) Reciprocal of the vertical shift factor, $1/b_{CO_2,PS}$, plotted against CO_2 pressure P_{CO_2}.

the segmental relaxation. If this is the case, CO_2 just accelerates the segmental relaxation without the mode broadening. This possibility is examined below.

From literature data,[22] the diffusion coefficient of CO_2 in PS at 110 °C is estimated to be $D = 1 \times 10^{-10}$ m^2 s^{-1} in the range of P_{CO_2} examined in this study. The segmental relaxation time τ_s estimated from the ε'' peak frequency is τ_s/s = 3×10^{-2} and 1×10^{-4} s for P_{CO_2}/MPa = 0 and 3.49, respectively (cf. Figure 8a). The average displacement of CO_2 during the segmental relaxation time, $(6D\tau_s)^{1/2}$, is estimated to be ∼5000 and 250 nm for $P_{CO_2} = 0$ and 3.49 MPa. This displacement is much larger than the segment size of PS (∼1 nm).[16] Thus, the very fast motion of CO_2 could have smeared the CO_2 concentration fluctuation before the dominant part of the PS segment relaxation occurs, thereby just accelerating this relaxation without affecting the mode distribution. This could be the case also for the PLA/CO_2 system, although no D data are available for CO_2 in PLA and we cannot quantitatively compare the CO_2 displacement and the PLA segment size.

As a back up of the above argument, we need to compare the displacement of ordinary solvents and the segment size. For tetracene being similar, in size, to ordinary solvents, the diffusion coefficient data in PS are available;[23] $D \cong 1 \times 10^{-16}$ m^2 s^{-1} at 110 °C. The corresponding displacement of tetracene, estimated from this D value and τ_s data ($= 3 \times 10^{-2} - 1 \times 10^{-4}$ s at 110 °C), is in a range between 0.2 and 4 nm, which is comparable to the PS segment size PS (∼1 nm). Thus, the motion of tetracene is not fast enough to smear the concentration fluctuation before the segmental relaxation occurs. This would be the case for ordinary solvents, demonstrating the difference between those solvent and CO_2.

4. Conclusion

We have performed the dielectric measurement for racemic DL-poly(lactic acid) (PLA) and polystyrene (PS) under the pressurized carbon dioxide (CO_2) to examine the effect of dissolved CO_2 on segmental relaxation of the polymers. We found that the dissolved CO_2 accelerates the segmental relaxation without affecting the relaxation mode distribution. This behavior was in contrast to the behavior of ordinary solvents (plasticizers) such as di-*n*-butyl phthalate (DBP), the acceleration of the segmental relaxation associated with the mode broadening.

The broadening of the segmental relaxation is related to the fluctuation of the solvent concentration that gives the frictional distribution to the segments. Diffusion data suggested that ordinary solvents move rather slowly so that they cannot smear this fluctuation in the time scale of segmental relaxation. In contrast, the small CO_2 molecules move rapidly to make this smearing so that they just accelerate the segmental relaxation without affecting the mode distribution. Thus, the difference of the effects of ordinary solvents and CO_2 on the segmental relaxation can be attributed to a difference of their mobilities.

Acknowledgment. This study was partially supported by a KAKENHI (Grant-in-Aid for Scientific Research) on Priority Area "Soft Matter Physics" and No. 19750182 and 20340112 from the Ministry of Education, Culture, Sports, Science, and Technology of Japan.

References and Notes

(1) Tomasko, D. L.; Li, H. B.; Liu, D. H.; Han, X. M.; Wingert, M. J.; Lee, L. J.; Koelling, K. W. *Ind. Eng. Chem. Res.* **2003**, *42*, 6431–6456.
(2) Nalawade, S. P.; Picchioni, F.; Janssen, L. *Prog. Polym. Sci.* **2006**, *31*, 19–43.
(3) Royer, J. R.; Gay, Y. J.; Desimone, J. M.; Khan, S. A. *J. Polym. Sci., Polym. Phys.* **2000**, *38*, 3168–3180.
(4) Kwag, C.; Manke, C. W.; Gulari, E. *J. Polym. Sci., Polym. Phys.* **1999**, *37*, 2771–2781.
(5) Areerat, S.; Nagata, T.; Ohshima, M. *Polym. Eng. Sci.* **2002**, *42*, 2234–2245.
(6) Park, H. E.; Dealy, J. M. *Macromolecules* **2006**, *39*, 5438–5452.
(7) Park, H. E.; Lim, S. T.; Laun, H. M.; Dealy, J. M. *Rheol. Acta* **2008**, *47*, 1023–1038.
(8) Ouchi, S.; Masubuchi, Y.; Shikuma, H. *Int. Polym. Process* **2008**, *23*, 173–177.
(9) Matsumiya, Y.; Inoue, T.; Watanabe, H.; Kihara, S.; Ohshima, M. *Nihon Reoroji Gakkaishi (J. Soc. Rheol. Jpn.)* **2007**, *35*, 155–161.
(10) Ren, J. D.; Adachi, K. *Macromolecules* **2003**, *36*, 5180–5186.
(11) Watanabe, H. *Macromol. Rapid Commun.* **2001**, *22*, 127–175.
(12) Pakula, T. Dielectric and Mechanical Spectroscopy - a Comparison. In *Broadband Dielectric Spectroscopy*; Kremer, F., Schönhals, A., Eds.; Springer: Berlin, 2003; Chapter 16, pp 597−623.
(13) Schönhals A.; Kremer, F. Theory of Dielectric Relaxation. In *Broadband Dielectric Spectroscopy*; Kremer, F., Schönhals, A., Eds.; Springer: Berlin, 2003; Chapter 1, pp 1−33.
(14) Liu, D. L.; Tomasko, D. *J. Supercrit. Fluids* **2007**, *39*, 416–425.
(15) The swelling of PLA (and PS) with CO_2 does not affect the dielectric data obtained with our cell having the fixed gap between the electrodes, as explained in the text. Nevertheless, it is informative to consider unrealistic cases: case 1 where the electrodes are freely mobile and the swollen material fully remained between the électrodes and case 2 where the material is affinely swollen between the mobile electrodes. The gap increases from L_0 (initial value before swelling) to $L_0 r_V$ and $L_0 r_V^{1/3}$ for the cases 1 and 2, respectively, with r_V (> 1) being the volume expansion ratio. The gap increase itself reduces, by factors of $1/r_V$ and $1/r_V^{1/3}$ for the case 1 and 2, the *apparent* dielectric intensity $\Delta\varepsilon_{app}$ uncorrected for this increase. Since the PLA concentration in the swollen material is given by $c = \rho_{ref}/r_V$, $\Delta\varepsilon_{app}$ becomes smaller than $\Delta\varepsilon_{ref}$ of neat PLA by factors of $1/r_V^2$ and $1/r_V^{4/3}$ for the cases 1 and 2, respectively. Thus, the reciprocal of the vertical shift factor is expressed as $1/b_{CO_2} = 1/r_V^2$ (for case 1) and $1/b_{CO_2} = 1/r_V^{4/3}$ (for case 2). Since $r_V = \rho_{ref}/c$, the b_{CO_2} data (= 0.93 for P_{CO_2} = 2.02 MPa at 48.5 °C) give c = 1.20 and 1.17 g/cm^3 for the cases 1 and 2, respectively. These c values may appear to be in an expected range. However, the linear decrease of $1/b_{CO_2}$ with P_{CO_2} (Figure 6b) gives anomalous P_{CO_2} dependence of c ($\propto P_{CO_2}^{1/2}$ and $\propto P_{CO_2}^{3/4}$ for the cases 1 and 2) being inconsistent with the *PVT* data.[14] The lack of the effect of swelling on the data measured with our cell can be confirmed also from this result.

(16) Inoue, T. *Macromolecules* **2006**, *39*, 4615–4618.
(17) Nakazawa, M.; Urakawa, O.; Adachi, K. *Macromolecules* **2000**, *33*, 7898–7904.
(18) Yada, M.; Nakazawa, M.; Urakawa, O.; Morishima, Y.; Adachi, K. *Macromolecules* **2000**, *33*, 3368–3374.
(19) Yoshizaki, K.; Urakawa, O.; Adachi, K. *Macromolecules* **2003**, *36*, 2349–2354.
(20) Inoue, T.; Uematsu, T.; Osaki, K. *Macromolecules* **2002**, *35*, 820–826.
(21) Floudas, G.; Reinsinger, T. *J. Chem. Phys.* **1999**, *111*, 5201–5204.
(22) Sato, Y.; Takikawa, T.; Takishima, S.; Masuoka, H. *J. Supercrit. Fluids* **2001**, *19*, 187–198.
(23) Cicerone, M. T.; Blackburn, F. R.; Ediger, M. *Macromolecules* **1995**, *28*, 8224–8232.